

Design and analysis on kinematics of the lap-polisher with planet movement for optical fiber end-face

Jun Wang · Yu-Shan Lu · Qi-Lin Shu · Jun Sun ·
Xiao-Jiao Zheng

Received: 9 August 2009 / Accepted: 26 January 2010 / Published online: 25 February 2010
© The Author(s) 2010. This article is published with open access at Springerlink.com

Abstract In order to obtain the effects of the kinematical state on the profile precision of the fiber-optic end-face in the process of lapping and polishing, a kinematical equation of the lap-polisher with planet movement is developed. Based on these equations and the tribological model of CMP, the dimensionless distribution of the material removal volume (DDMRV) and the trajectories of abrasive grains cutting on the lap-polisher are numerically simulated with the way of stochastic abrasive grains. Then, the effects of the parameters of the lap-polisher on the uniformity of the DDMRV and the trajectory on the optical fiber end surface are discussed, and the results are that the DDMRV and the trajectory of abrasive grains have a rather better value when the length L of the planet carrier and the rotational speed n_1 of the ring gear are increased and the rotation speed n_H of the planet carrier is chosen in an advisable parameter region.

Keyword Lapping and polishing · Optical fiber connectors · Optical fiber lens · Material removing rate · Uniformity

1 Introduction

Optical fiber connectors and optical fiber lens are the most important optical transmission and coupling components in

the area of optical fiber communication, the fabrication quality of their macro- and micro-surface directly affects the coupling efficiency and transmission reliability. Therefore, the manufacturing processes of the optical fiber connectors and the fiber-optic lens have become more and more important. In the fabricating area of the fiber-optic connectors and optical fiber lens, lapping and polishing are one of the most important ways which can produce the connector and the lens with perfect surface morphology. Many scholars have carried out research and analysis on this topic and have achieved encouraging results [1–6]. However, achieving the best effect of lapping and polishing through the reasonable design of the movement parameters of lap-polisher is still a technically difficult problem. In the process of lapping and polishing, the material removal rate can be described by Preston equation [7] and Liu model [8], that is, the material removal rate of lapping and polishing points in the workpiece surface is proportional to the contact pressure and relative velocity of those points. Therefore, for the lapping and polishing of fiber-optic connectors and optical fiber lens end-face, if the contact pressure and the average relative velocity of every point of the end surface are different, the volume of material removed from the end-face will be different after a certain amount of lapping and polishing time, which will create a corresponding end profile error [9–12]. However, in the process of lapping and polishing, in order to meet the requirements of macro surface precision and micro-texture of the fiber and connector end-face, it is aimed to keep the average relative velocity distribution or the distribution of friction length over the fiber and connector constant in a given processing cycle. At the same time, if the curve trend of the abrasive trajectory is gentle or curvature of the trajectory is low, the polishing pad or lapping platen will not produce the abnormal wear and the reasonable surface

J. Wang · Y.-S. Lu (✉) · Q.-L. Shu
School of Mechanical Engineering, Shenyang Ligong University,
Shenyang 110159, China
e-mail: yushan_lu@yahoo.com.cn

J. Sun · X.-J. Zheng
School of Traffic & Mechanical Engineering,
Shenyang Jianzhu University,
Shenyang 110168, China

profile of lapped and polished workpiece can be obtained [12]. Therefore, to get the best effect of the lapping and polishing processes, designing rationally the movements parameters of the lap-polisher for fiber optical end is one of the key technological points in the lapping and polishing of optical fiber end. In light of the above issues, the kinematics of the lap-polisher with planet movement will be simulated and analyzed by using suitable tribological theories in this article.

2 Transmitting mechanism of the lap-polisher for optical fiber end-face

Figure 1 shows the transmission mechanism of the lap-polisher for fiber optical connector end and fiber optical lens based on planet movement mechanism. Its movement setup is mainly composed by the platen carrier, ring gear, planetary gear, and so on. Two motors drive the planet carrier shaft and ring gear shaft for movement by timing belt, respectively. The lap-polishing platen is assembled in the planetary gear. In this way, the abrasive grits on the surface of the lap-polishing platen can form a complex cutting movement trajectory. In the lapping or polishing of fiber end-face, optical fiber connector or optical fiber lens surface are pressed to the lap-polishing platen surface, and grinded and cut by the abrasive grains over lap-polishing platen or polishing pad. This kind of lap-polishing movement can resolve optical fiber entanglement in processing.

3 Kinematical equation of the lap-polisher

Figure 2 shows the movement principle of lapping and polishing with planet movement. Table 1 shows its relative movement parameters. In order to establish the kinematical equations of the lap-polisher, the coordinate system XOY is

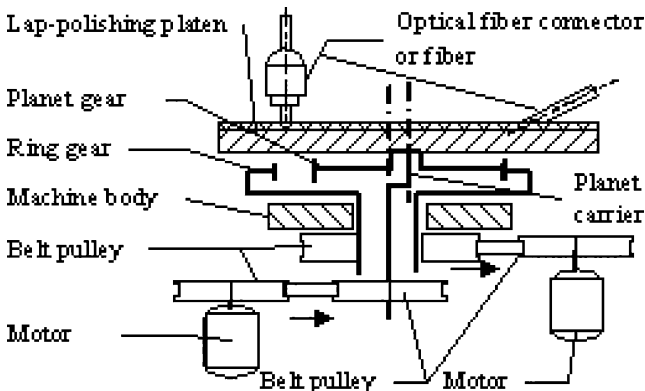


Fig. 1 Mechanism principle of the lap-polisher for optical fiber end

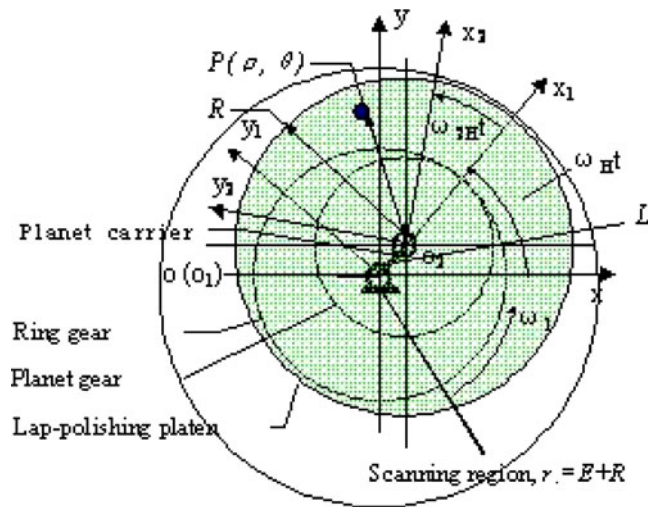


Fig. 2 Schematic of kinematic geometry of the lap-polisher with planet movement for optical fiber end

fixed in its bed, the first moving coordinate system $X_1O_1Y_1$ is fixed in the platen carrier, and the second moving coordinate system $X_2O_2Y_2$ is fixed in the planetary gear or the lap-polishing platen. In the process of lapping and polishing, the material removal is achieved by depending on the friction and cutting of abrasive grits. Assuming that point $P(\rho, \theta)$ is an abrasive grit point on lap-polishing platen, using the principle of coordinate transformation and kinematics, the kinematical equations of the point $P(\rho, \theta)$ can be obtained, which are derived as follows:

If the location of random abrasive point $P(\rho, \theta)$ in the coordinate system $X_2O_2Y_2$ is

$$\begin{cases} x_{2p} = \rho \cos(\omega_{2H}t + \theta) \\ y_{2p} = \rho \sin(\omega_{2H}t + \theta) \end{cases} \quad (1)$$

By coordinate transformation theory, the position equation of a random abrasive point $P(\rho, \theta)$ in the coordinate system $X_1O_1Y_1$ is

$$\begin{cases} x_{1p} = \rho \cos(\omega_{2H}t + \theta) + L \\ y_{1p} = \rho \sin(\omega_{2H}t + \theta) \end{cases} \quad (2)$$

In Eqs. 1 and 2, ρ and θ are the polar coordinates location of an abrasives grit point $P(\rho, \theta)$. L is the tie bar length, ω_{2H} is the relative rotating frequency of lap-polishing platen, by coordinate rotation theory, Eq. 2 is transformed and $\omega_{2H} = \omega_2 - \omega_H$ is substituted into Eq. 2, and then the trajectory equation of an abrasive grit point $P(\rho, \theta)$ in the coordinate system XOY can be expressed as follows:

$$\begin{bmatrix} x_p \\ y_p \end{bmatrix} = \begin{bmatrix} \cos(\omega_2 t + \theta) & \cos(\omega_H t) \\ \sin(\omega_2 t + \theta) & \sin(\omega_H t) \end{bmatrix} \begin{bmatrix} \rho \\ L \end{bmatrix} \quad (3)$$

Table 1 Movement parameters of the lap-polisher for optical fiber end-face

Movement parts	Rotation speed		Rotation frequency	
	Absolute	Relative	Absolute	Relative
Ring gear	n_1	$n_{1H} = n_1 - n_H$	ω_H	$\omega_{1H} = \omega_1 - \omega_H$
Planet gear	n_2	$n_{2H} = n_2 - n_H$	ω_2	$\omega_{2H} = \omega_2 - \omega_H$
Planet carrier	n_H		ω_H	
Relation of parameters	$n_2 = [z_1 n_1 + (z_2 - z_1) n_H] / z_2$; z_1 is teeth number of ring gear, z_2 is teeth number of planet gear, $\omega = \pi n / 30$			

In Eq. 3, ω_2 and ω_H are the absolute frequency of planetary gear and platen carrier, respectively. By the kinematical theory, the differential coefficient of Eq. 3 to the time t is the velocity equation of an abrasive grit point $P(\rho, \theta)$, it can be expressed as:

$$\begin{bmatrix} V_{xp} \\ V_{yp} \end{bmatrix} = \begin{bmatrix} -\sin(\omega_2 t + \theta) & -\sin(\omega_H t) \\ \cos(\omega_2 t + \theta) & \cos(\omega_H t) \end{bmatrix} \begin{bmatrix} \rho \omega_2 \\ L \omega_H \end{bmatrix} \quad (4)$$

$$V_p = \sqrt{V_{px}^2 + V_{py}^2}$$

According to the actual geometrical structure of the lap-polisher, the ranges of the radius ρ and initial angle θ of point $P(\rho, \theta)$ are $\rho \in [0, 75]$, $\theta \in [0, 2\pi]$, respectively.

4 Model of dimensionless distribution of material removal volume

There are many models which describe material removal rate during lapping and polishing, for the example experiment model, the wear model and analytical model [7, 8, 13–17]. Based on these models, it can be seen that the material removal rate Z'_w is directly proportional to the polishing relative velocity V . If the average abrasive grit numbers are n_g in a unit polished area, under the condition of an invariant polishing contact pressure, the average material removal rate $Z'_w(t)$ is as follows [18]:

$$Z'_w(t) = 0.25 C a_p^2 \tan\left(\frac{\beta_p}{2}\right) V_p(\rho, \theta, t) n_g \quad (5)$$

Where a_p is the average cutting depth of abrasive grits, β_p is the average top angle of abrasive grits, thus the

material removal rate $Z'_{wp}(t)$ of a single abrasive grit is as follows:

$$\begin{aligned} Z'_{wp}(t) &= 0.25 C a_p^2 \tan\left(\frac{\beta_p}{2}\right) V_p(\rho, \theta, t) \\ &= 0.25 C a_p^2 \tan\left(\frac{\beta_p}{2}\right) \sqrt{V_{xp}^2(\rho, \theta, t) + V_{yp}^2(\rho, \theta, t)} \end{aligned} \quad (6)$$

where C is a coefficient that depends on the geometry and physical property of the polishing pad and abrasive material, and the physical and chemical property of polishing slurry as well as polishing pressure.

During the lapping and polishing of optical fiber end-face, as shown in Fig. 2, the optical fiber connector or lens are installed in the scanning region of the lap-polishing platen. Since the lapping and polishing undergoing any point in the same radius on the scanning region is the same in a polishing period, the distribution of the material removal volume of lapped and polished region is an axle symmetrical. For obtaining the model of the material removal distribution on lapping and polishing optical fiber end-face, firstly, the scanning radial interval $[0, r_1]$ is separated into N intervals $[\frac{i}{N}r_1, \frac{i+1}{N}r_1)$, $i = 0, 1, 2, \dots, N - 1$. secondly, a large numbers of abrasive grain points $p_j (p_j, \theta_j)$ which satisfy with the random statistical law and $\rho_j \in [0, R]$, $\theta_j \in [0, 2\pi]$, $j = 1, 2, \dots, M$. are chosen, and then by the use of Eqs. 4 and 6 and letting $x_{p_j}(\rho_j, \theta_j) = 0, y_{p_j}(\rho_j, \theta_j) = r_i$ of Eq. 3, where $r_i \in [\frac{i}{N}r_1, \frac{i+1}{N}r_1)$. Therefore, the material removal volume $Z_{wi} \sum$ in $r_i \in [\frac{i}{N}r_1, \frac{i+1}{N}r_1)$ and the sum total $Z_{wi} \sum \sum$ of the material removal volume of scanning radial region in a lapping or polishing period T can be expressed as follows:

$$\begin{cases} Z_{wi} \sum = \left[0.25 C a_p^2 \tan\left(\frac{\beta_p}{2}\right) \right] \sum_{j=1}^M \sum_{k=0}^K \sqrt{V_{xp}^2(\rho_j, \theta_j, t_{jik}) + V_{yp}^2(\rho_j, \theta_j, t_{jik})} \Delta t \\ Z_{wi} \sum \sum = \left[0.25 C a_p^2 \tan\left(\frac{\beta_p}{2}\right) \right] \sum_{i=0}^{N-1} \sum_{j=1}^M \sum_{k=0}^K \sqrt{V_{xp}^2(\rho_j, \theta_j, t_{jik}) + V_{yp}^2(\rho_j, \theta_j, t_{jik})} \Delta t \end{cases} \quad (7)$$

where K is the cut frequency of the interval $[\frac{j}{N}r_1, \frac{j+1}{N}r_1)$, which is done by j th abrasive grit.

From Eq. 7, the dimensionless distribution of the material removal volume (DDMRV) $Z_{rw}(i)$ on scanning region can be gained. It can be expressed as follows:

$$Z_{rw}(i) \Big|_{x_p(\rho,\theta)=0, y_p(\rho,\theta)=r_i} = \frac{Z_{wi} \sum}{Z_{wi} \sum \sum} = \frac{\sum_{j=1}^M \sum_{k=0}^K \sqrt{V_{xp}^2(\rho_j, \theta_j, t_{jik}) + V_{yp}^2(\rho_j, \theta_j, t_{jik})} \Delta t}{\sum_{i=0}^{N-1} \sum_{j=1}^M \sum_{k=0}^K \sqrt{V_{xp}^2(\rho_j, \theta_j, t_{jik}) + V_{yp}^2(\rho_j, \theta_j, t_{jik})} \Delta t} \tag{8}$$

Where t_{jik} is the time, which the j th abrasive grit has passed through the i th interval $[\frac{j}{N}r_1, \frac{j+1}{N}r_1)$ at k time.

Since the optical fiber lens or connectors is installed in the scanning region during lapping and polishing, the material removed distribution $Z_{rw}(i)$ on the scanning region can reflect the material removal distribution on the optical fiber end-face.

5 Kinematical simulating on lapping and polishing process

In the process of lapping and polishing for optical fiber end-face, the abrasives as a media is larded between polishing pad and optical fiber end-face, and embedded in the surface of polishing pad as a specific “point” to achieve the cutting of the workpiece. However, the process is achieved by a group of abrasive grits in a random manner, which is subject to the laws of statistics [13, 14]. $P(\rho, \theta)$ is the uniform distribution of grits in $X_2O_2Y_2$ or $2\pi mg\rho$ in polar coordinate system.

Therefore, it is more realistic that for lapping and polishing, we consider the average height of abrasive grits and simulate the whole process by considering the trajectory of an average abrasive point than consider the distribution of the average relative velocity in the processing region using the Preston equation [7]. However, the Monte Carlo method in mathematics provides a way of randomized trial to solve specific problems [12]. According to the Monte Carlo method, when making full use of the statistical process in a random experiment and combining with the computer pseudo-random number, this kind of simulated study is possible. The Matlab software will also be used for processing of calculation and simulation.

5.1 Simulation and analysis of abrasive cutting trajectory

The relevant research on lapping and polishing has shown that the trajectory curve formed by abrasives point movement impact directly on processing efficiency, the processed workpiece surface texture, as well as the wear status of polishing pad or lapping platen, and so on [9–12, 17, 18], the

uniform distribution of the complex but smooth cutting trajectory is the most advantageous for an ideal process. Therefore, in parameter region $\rho \in [0, 75], \theta \in [0, 2\pi]$, by simulating the trajectory of random abrasive $P(\rho, \theta)$ point using Eq. 3 and inspecting the trajectory of a single abrasives point and the multi-points trajectory superposition, reasonable motion parameters will be obtained.

Figures 3 and 4 show typical single point trace and multi-point trajectories, respectively, which are obtained by computer simulation. From simulation results, it is seen that the abrasive trajectory is cross-arc form. The type, shape and position of trajectory curves change constantly with the

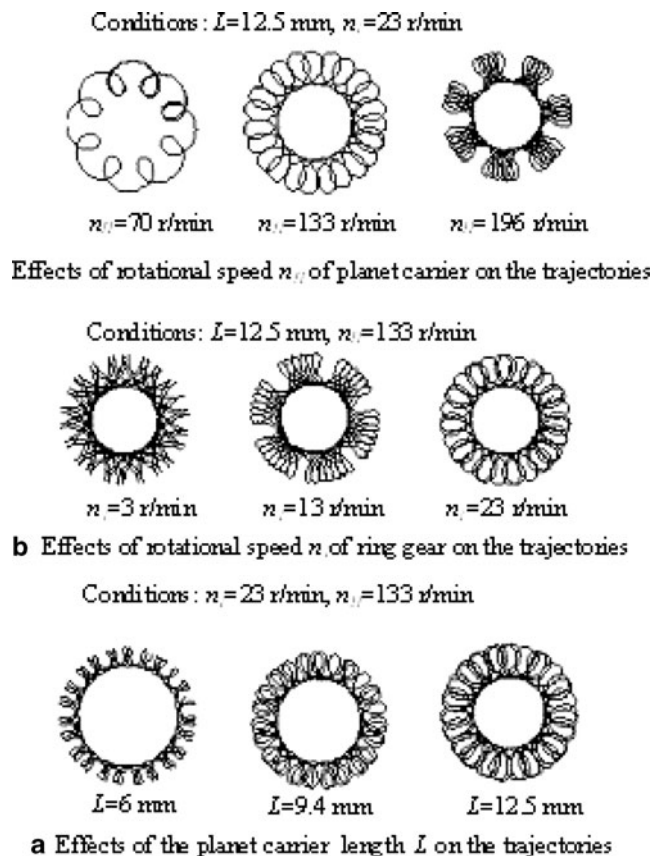


Fig. 3 Trajectory of an abrasive grain for different kinematical parameters

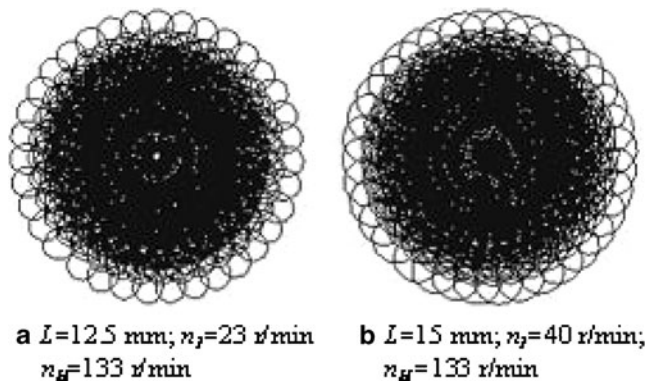


Fig. 4 Trajectories of many abrasive grains

change of the planet carrier length L , the rotating speed n_I ($n_I=30\omega_I/\pi$) of ring gear and the rotating speed n_H ($n_H=30\omega_H/\pi$) of planet carrier, which shows the complexity of the trajectory change and that the trajectory of points at different radius are different. From Eq. 3, it can be seen that since the trajectory curve function is a periodic function, to make the lapping platen or polishing pad wear uniformly, the periodic superposition of the lapping and polishing trajectory over optical fiber connectors or optical fiber lens end should be avoided. Theoretically, when the lapping or polishing time is infinite, to make sure the lapping and polishing trajectories are not superposed periodically, the transmission ratio of the lap-polisher should be chosen to be an irrational number [11, 12]. Therefore, for achieving a reasonable trajectory, it is necessary to adjust rationally the above movement parameters. For improving material removal uniformity and preventing the abnormal wear of the polishing pad or lapping platen in the lapping and polishing process, it can be shown that the result is better if the curve trend of the abrasive trajectory is gentle or curvature of the trajectory is low. But, for the general trend

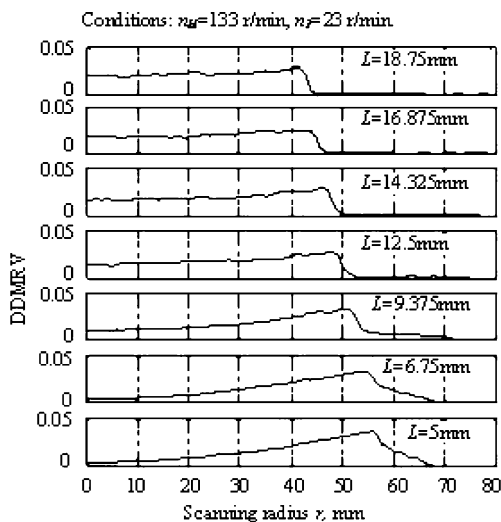


Fig. 5 The effects of the length L of the planet carrier on the DDMRV

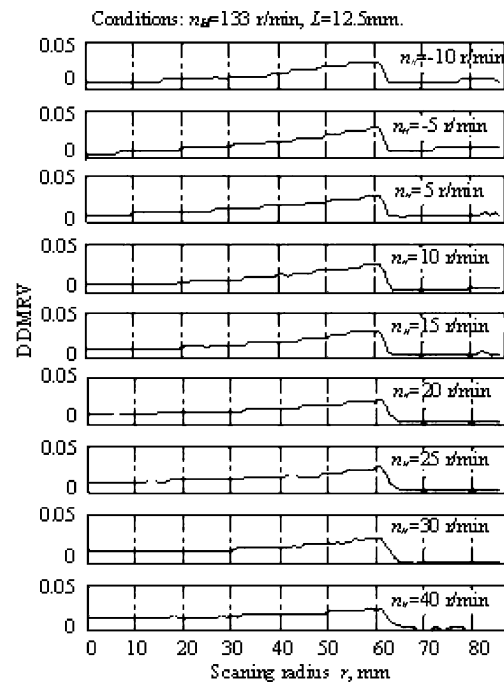


Fig. 6 The effects of the rotational speed n_1 of the ring gear on the DDMRV

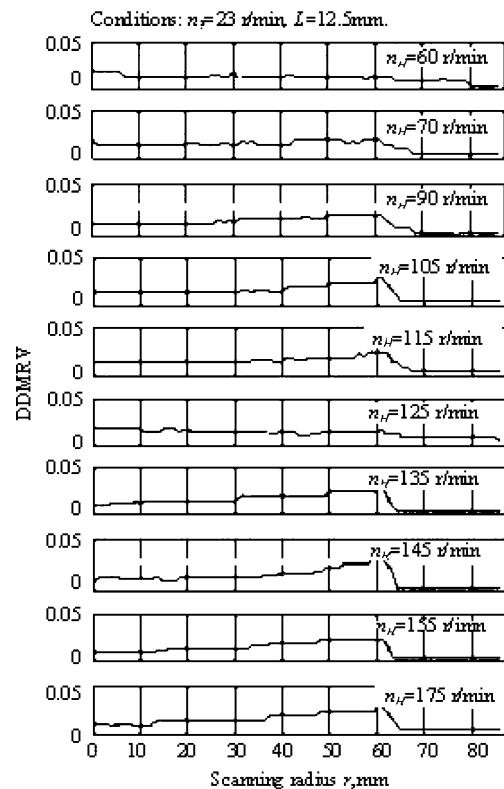


Fig. 7 The effects of the rotation speed n_H of the planet carrier on the DDMRV

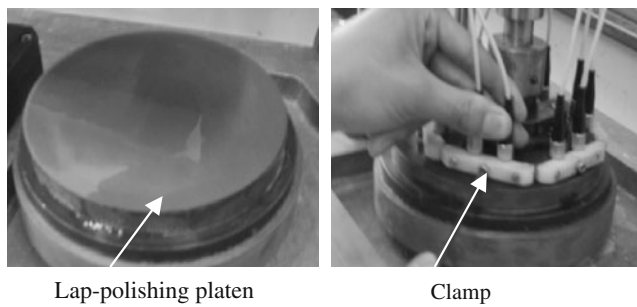


Fig. 8 Lap-polishing platen and clamp of the lap-polisher for optical fiber connectors

of the trajectory points on the lapping platen surface, in order to make abrasive point trajectory gentle, it is necessary to increase the planet carrier length L , increase the rotating speed n_1 of the ring gear, and properly choose the rotating speed n_H of the planet carrier, and so on.

5.2 Simulation on the effects of movement parameters on material removal distribution

In the processing of lapping and polishing, based on the Preston equation [7], it can be seen that under the uniform contact pressure distribution on polished and lapped surface, the uniformity of distribution of the material removal rate from the workpiece surface is dependent on the uniformity of distribution of relative velocity between workpiece and the lap-polishing platen [9]. Theoretically, in the lapping and polishing of optical fiber end-face, it is assumed that the instantaneous relative velocity over optical fiber end-face can be kept constant or a subject to a minimal variation, which can obtain the best processing of the workpiece surface. But, in fact, due to the constraint of the structural design of the mechanical transmission, obtaining this effect is very difficult, and so in the actual production, it is assumed that if the designed lap-polisher can make the average relative velocity of workpiece surface points constant in one polishing cycle T by adjusting the relevant movement parameters, then the same effects will be achieved. Based on the tribological model of chemical mechanical polishing, the volumetric material removal over a lapped or polished point is the cumulative total of what is achieved by the cutting and rubbing by a large number of

abrasive grits in a given polishing cycle T , and it is proportional to the relative friction cutting length [8, 9, 12]. So if the relative friction cutting length of processed points on workpiece surface is uniformly distributed, it will be possible to get the flattest processed surface. However, for polishing and polishing surface, the larger the material removal volume at any of the polished or lapped point is, the larger the sunken depth of workpiece surface is, and vice versa.

In actual simulation process, Eq. 8 can be used for analyzing the non-uniformity of the DDMRV, and the material removal distribution of scanned round region can be obtained when the non-uniformity of DDMRV is made out in the Y axis direction in a given period T . In this way, the region that optical fiber connector or fiber-optic lens can be installed and the effects of related movement parameters on the profile errors of polished or lapped optical fiber end-face are also determined when machined workpiece is assembled in different installation location. Therefore, through discussing the DDMRV change in scanning radius $r \in [0, r_1 = L + R]$ region, the best structure and process parameters for lap-polisher can be obtained.

For obtaining the DDMRV of the lap-polisher in the range of $r \in [0, r_1 = L + R]$, based on the theories of Section 4 and by the use of the Eqs. 3, 4, 7 and 8, the DDMRV $Z_{rw}(i)$ will be simulated by computer. The results of the DDMRV $Z_{rw}(i)$ are expressed as follows:

Figures 5, 6, and 7, respectively, show that the effects of the planet carrier length L , the rotating speed n_1 of the ring gear, as well as the rotating speed n_H of planet carrier on DDMRV, it can be seen that the DDMRV in the center of scanned region is even, but, from Fig. 5, as can be seen, the uniformity of the DDMRV is increasing with the increasing of the planet carrier length L and the uniform region is decreasing. In Fig. 5, the reason which make the uniform region smaller with the increasing of the planet carrier length L is that the region $r \subseteq [R - L, R + L]$ is discontinuously scanned by the lap-polishing platen, where $[R - L, R + L] \in [0, r_1 = R + L]$. The material removal volume is increasing in the radial direction in the interval. From Fig. 6, it can be seen that the uniformity of the DDMRV is improved with the increasing of the rotational speed n_1 of ring gear from -15 r/min to 40 r/min in the entire scanned region, and the increasing phenomenon

Table 2 Experimental conditions for the lapping and polishing of optical fiber connectors

Process	Stage 1	Stage 2	Stage 3
Lapping film and polishing pad	9 μm diamond film	3 μm diamond film	0.01 μm SiO ₂ film
Lapping and polishing pressure	0.45 MPa	0.3 MPa	0.3 MPa
Lapping and polishing period	80 s	80 s	70 s
Lapping and polishing reagent	Water	Water	SD6-2D

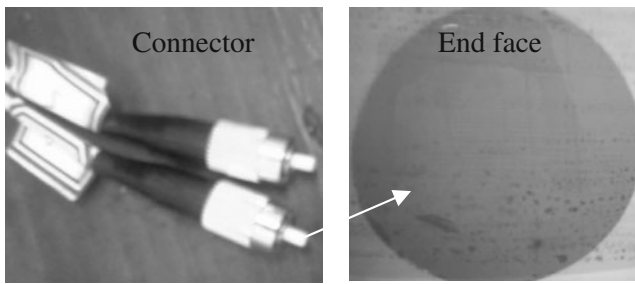


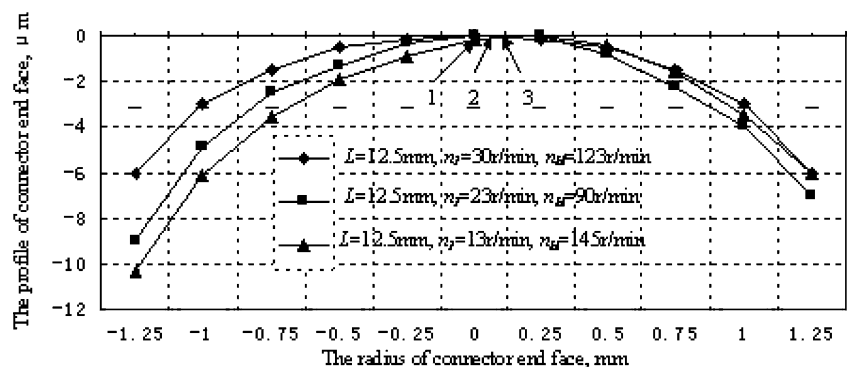
Fig. 9 Polished connector and its end-face

occurs in the scanned region of interval $r \subseteq [0, 60]$, but the material removal volume is increasing sharply when the radius is $r > 60$ mm. For Fig. 7, two regions making the DDMRV relative uniform have occurred due to the change of the rotating speed n_H of the planet carrier. That is, the interval $n_H \in (65, 85)$ and $n_H \in (110, 135)$.

As a result, in the actual process of lapping or polishing and designing machine, the fiber optical lens and connectors should be assembled in the near center region or $r \subseteq [45, 60]$ mm of the scanned region as far as possible. Choosing the right length L and rotational speed n_H of planet carrier, increasing the rotational speed n_I of the ring gear can improve the uniformity of the DDMRV of lapped and polished surface.

According to simulation results, the lap-polisher for the FC-type optical fiber connector end-face has been designed. Its lap-polishing platen and the jig are shown in Fig. 8. In this designing, the planet carrier length L is 12.5 mm, the teeth number Z_1 of ring gear is 53, the teeth number Z_2 of planetary gear is 33, the gear modulus m is 1.25, the diameter of lap-polishing platen is $\Phi 150$ mm, optical fiber connectors are distributed in the clamp of circumferential diameter $\Phi 120$ mm, 12 optical fiber connectors are polished at every time. In the lapping and polishing experiment, a rubber pad is affixed on lap-polishing plate, and then the diamond paper or polishing pad is affixed on the rubber pad. The hardness of the rubber pad is 70 and its thickness is 3 mm. The profile of the end-face of the connector is measured by numeric tool microscope JX4B. Table 2 shows experimental conditions. Figure 9 shows the lapped and

Fig. 10 The profile of lapped and polished end-face of optical fiber connector



polished connector and its end-face. Figure 10 shows the end-face profiles of the lapped and polished connectors with the different machining parameters. From Fig. 10, it can be seen that the end-face profiles of the connector is spherical, and the spherical center is inconsistent with the center of the connector when the lapping and polishing parameters are $L=12.5$ mm, $n_1=23$ r/min, and $n_H=90$ r/min, and $L=12.5$ mm, $n_1=13$ r/min, and $n_H=145$ r/min. The spherical profile of the connector is created by the non-uniformity of the contact pressure distribution of lapping and polishing [12, 16], and the deviation of the spherical center of the connector is produced by the non-uniformity of the DDMRV. By the experiment of the lapping and polishing of the connectors, it is ensured that the macro-profile and micro-texture of polished connector end meet the IEC standard.

6 Conclusions

Through the studies of kinematical modeling and calculating simulation on the lap-polisher for optical fiber end-face, the conclusions can be drawn as follows:

1. By selecting the appropriate length L of the planet carrier, and the rotating speed n_H of planet carrier, as well as the greater rotating speed n_I of ring gear, the relative movement trajectory curve extent between lap-polishing platen and optical fiber end can become flatter and the DDMRV become more uniformly, and the profile accuracy of polished and lapped optical fiber end-face will also be improved.
2. In the actual process of lapping and polishing, and designing clamp, the optical fiber connector or lens should assemble in the near center region which is scanned by the lap-polishing platen, that is, in its radius $r \leq R-L$ as far as possible.
3. From the tribological theory of chemical mechanical polishing, the design and analysis of the lap-polisher for optical fiber end-face based on the method of random abrasive points is feasible.

Acknowledgments The authors gratefully acknowledge the financial support provided by Liaoning Province Science Foundation of the People Republic of China (Grant No. 20072008).

Open Access This article is distributed under the terms of the Creative Commons Attribution Noncommercial License which permits any noncommercial use, distribution, and reproduction in any medium, provided the original author(s) and source are credited.

References

1. Yousef AG, Jayantha K (2004) Experimental determination of optimum parameters for nano-grinding of optical fibre end faces. *Int J Mach Tools Manuf* 44:725–731
2. Kanda T, Misuhashi M, Ueda T, Toyohara A, Yamamoto K (1995) New micro-finish surface technology for the fabrication of optical device end faces. *Proc SPIE* 2576:84–91
3. Yin L, Huang H, Chen WK, Xiong Z, Liu YC, Teo PL (2004) Polishing of fiber optic connectors. *Int J Mach Tools Manuf* 44:659–668
4. Yin L, Huang H, Chen WK (2005) Influences of nanoscale abrasive suspensions on the polishing of fiber-optic connectors. *Int J Adv Manuf Technol* 25:685–690
5. Huang H, Chen WK, Yin L (2004) Micro/meso ultra precision grinding of fiber optic connectors. *Precis Eng* 28:95–105
6. Liu DF, Duan JA, Zhong J (2006) Motion analysis of lapping machine for end face of optical fiber connector. *Optics and Precision Engineering* 14:159–166 (in Chinese)
7. Preston FW (1927) The theory and design of glass polishing machines. *J Soc Glass Technol* 11:214–256
8. Liu CW, Dai BT, Tseng WT, Yeh CF (1996) Modeling of the wear mechanism during chemical–mechanical polishing. *J Electrochem Soc* 143:716–721
9. Hocheng H, Tsai HY, Tsai MS (2000) Effects of kinematical variables on non-uniformity in chemical mechanical planarization. *Int J Mach Tools Manuf* 40:1651–166
10. Tso PL, Wang YY, Tsai MJ (2001) A study of carrier motion on a dual-face CMP machine. *J Mater Process Technol* 116:194–200
11. Uhlmann E, Ardel TT (1999) Influence of kinematics on the face grinding process on lapping machines. *CIRP Annals* 48(1):281–284
12. Lu YS (1998) Theoretical and experimental researches on the ultraprecision plane lapping and polishing of thin workpiece. Ph. D. dissertation, School of Mechanical Engineering and Automation Northeastern University, Shenyang, (In Chinese)
13. Xie YS, Bhushan B (1996) Effects of particle size, polishing pad and contact pressure in free abrasive polishing. *Wear* 200:281–295
14. Ahmadi G, Xia X (2001) A model for mechanical wear and abrasive particle adhesion during the chemical mechanical polishing process. *J Electrochem Soc* 148:G99–G109
15. Seok J, Sukam CP, Kim AT, Tichy JA, Cale TS (2003) Multiscale material removal modeling of chemical mechanical polishing. *Wear* 254:307–320
16. Horng TL (2008) Modeling and simulation of material removal in planarization process. *Int J Adv Manuf Technol* 37:323–334
17. Chiu JT, Lin YY (2008) Modal analysis of multi-layer structure for chemical mechanical polishing process. *Int J Adv Manuf Technol* 37:83–91
18. Yasui H, Suzuki Y, Kobayashi T (1997) Studies on roll-off-less polishing of magnetic disk substrate. *Journal of the JSPE* 63:404–409